Prediction of the Phase Diagram of Rigid C_{60} Molecules

Ailan Cheng and Michael L. Klein

Department of Chemistry and Laboratory for Research on the Structure of Matter, University of Pennsylvania, Philadelphia, Pennsylvania 19104-6323

Carlo Caccamo

Dipartimento di Fisica, Universita degli Studi Messina, C.P. 50, 98166 S. Agata di Messina, Italy

(Received 10 May 1993)

An integral-equation approach combined with molecular dynamics simulations based on the Girifalco spherical intermolecular potential has been used to predict the phase diagram for rigid C_{60} molecules. The boundary of the liquid-vapor coexistence region and the location of freezing and melting lines have been sketched out. The liquid phase is only observed in a very narrow temperature range compared with atomic systems (e.g., the rare gases). Unfortunately, the dense fluid is predicted to exist above ~ 1800 K, which is sufficiently high that the C_{60} molecule may be unstable.

PACS numbers: 64.70.Dv, 61.46.+w, 64.70.Fx

The discovery of an efficient synthesis of fullerenes has stimulated tremendous interest in this material [1]. To date, most studies have focused on the properties of the solid phases. The low-temperature structure is identified to be cubic $Pa\bar{3}$ with orientationally ordered molecules [2,3]. At room temperatures, C_{60} molecules are known to undergo hindered rotation [2,4,5]. Higher-temperature data are sparse. Knowledge of the phase diagram of C_{60} is not only of intrinsic theoretical interest, but also relevant to the optimization of the purification procedures [1]. The structure of the liquid is of considerable interest [6].

We have employed a refined integral-equation theory [7] and molecular dynamics (MD) simulations in an effort to predict the high-temperature behavior of C_{60}. Specifically, we have carried out a series of constant-pressure and constant-volume simulations using Girifalco's intermolecular potential model [8] for rigid C_{60} molecules in order to map out the high-temperature phase diagram. This study has enabled us to sketch the melting and freezing lines and the boundary of the liquid-vapor coexistence region. The integral-equation calculations and simulation results suggest that the triple point should occur around $T \approx 1800$ K. The main features of the predicted phase diagram are also compared with those of Lennard-Jones particles [9–11]. The triple point temperatures turn out to be in fair accord; however, there seems to be a significant difference in the liquid-vapor coexisting region, which we attributed to the much stiffer repulse wall, and the relatively narrower potential well in the Girifalco potential as compared with the Lennard-Jones (12-6) potential.

Earlier studies have established that a pair-wise additive carbon-carbon (C-C) Lennard-Jones potential gives a good description of the room temperature rotator phase [12]. Also, the assumption that pairs of carbon atoms on different molecules are interacting via Lennard-Jones potentials with parameters $\epsilon_{C\text{-}C} = 33$ K and $\sigma_{C\text{-}C} = 3.469$ Å produces a reasonable fit to the lattice constant and heat of sublimation [8]. The present study concentrates on a much higher temperature regime, where one would expect that molecules rotate even more freely. Therefore, it is to our advantage to ignore the internal structure of the C_{60} molecules; an approximation that saves a tremendous amount of computer time. Following Girifalco's work [8] the interaction is distributed uniformly on a sphere of radius $r_0 = 3.55$ Å with the same integrated density as in a 60-site model. The interaction between two C_{60} molecules can be integrated over the two interacting spheres to yield an analytic form for the intermolecular potential. The resulting potential well depth of two interacting C_{60} spheres is 3194 K with the energy minimum at 10.06 Å. This sphericalized C_{60} potential model with only one interaction site allows us to easily carry out MD simulations on large systems. In practice, we have mostly used 864 sphericalized C_{60} molecules. We have confirmed by direct calculation that the center-of-mass pair distribution function $g(r)$ for the full 60-site model [12] is essentially identical with that from the sphericalized Girifalco potential at the same density and temperature (see Fig. 1). Thus for the remainder of this Letter we will only be dealing with Girifalco's potential.

The integral equation calculations we employed are based on the Zerah and Hansen [7] closure of the Ornstein-Zernike equation, denoted HMSA because it bridges between the well known hypernetted chain (NHC) and the soft mean spherical approximation (SMSA). The theory contains an adjustable parameter which allows one to impose thermodynamic consistency between the virial and compressibility equation of state. The HMSA has recently been successfully applied for the determination of the phase diagram of both the one- and two-component Lennard-Jones (LJ) fluid [13,14]. In particular, for the one-component LJ fluid, it has been shown [14] that both the liquid-vapor *and* the freezing line can be determined with quantitative agreement with the simulation data. The freezing line was determined by applying a freezing criterion recently proposed by Gia-

0031-9007/93/71(8)/1200(4)$06.00

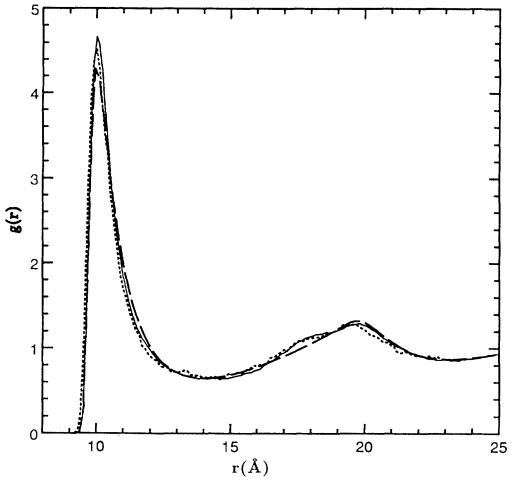

FIG. 1. The center-of-mass pair distribution functions, $g(r)$, at $V=637.7$ cm^3/mol and $T=1850$ K. The solid line is the MD result from the Girifalco sphericalized potential [8] and the dotted curve is from the full 60-site pair-wise additive atom-atom potential model [12]. The dashed curve is from integral-equation calculations using Girifalco's potential.

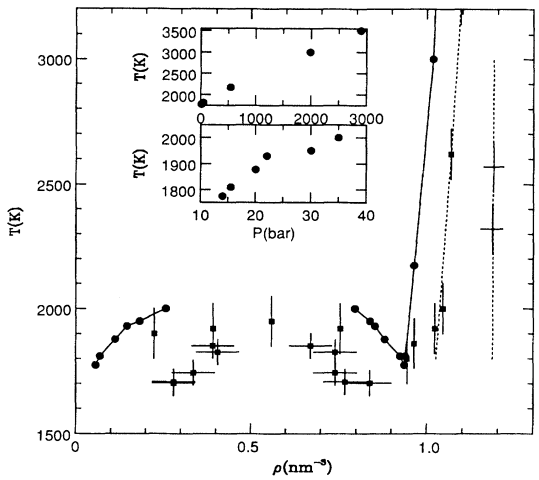

FIG. 2. The T-ρ phase diagram predicted by the MD simulation (squares and dotted lines) and HMSA theory (solid circles). The inset shows the HMSA T-P freezing line (upper) and the liquid-vapor coexistence line (lower).

quinta and co-workers [15,16], which rests on the analysis of the contribution of multiparticle correlations to the entropy of the fluid. A similar approach to that reported in Ref. [14] has been adopted here for the sphericalized Girifalco C_{60} potential. In practice, the HMSA needs to be solved along a series of isothermal and isochoric paths, starting from the zero-density limit, in order to be able to estimate the entropy and chemical potential of the system and hence draw the freezing and the liquid-vapor coexistence line.

In general, the most interesting questions related to the phase diagram concern the density of the liquid at melting, the location of the freezing line, and the boundary of vapor-liquid coexisting region. These issues were explored by carrying out constant-volume MD simulations guided by the prediction of the HMSA calculations. Figure 1 also compares the $g(r)$ function from an HMSA calculation (dashed line) at $V=637.7$ cm^3/mol and $T=1850$ K with the results of constant-volume MD simulations under the same conditions. In the third nearest neighbor region ($r\sim 18$ Å), simulation curves show a hint of a solid or glasslike feature. This is due to the presence of some solid clusters in the simulation system.

Simulations at several densities have been performed for increasing termerature with fixed number density. At $T\approx 1500$ K for $\rho=1.023$, 1.045, 1.067, and 1.095 nm^{-3}, solid C_{60} coexists with the liquid phase. The $g(r)$ functions, mean-square displacements, and time-dependent trajectory plots all confirmed this picture. As the temperature is raised, solid and liquid remain in coexistence. Gradually, the solid component shrinks and the liquid region expands with increasing temperature. Eventually, the solid features disappear and the fluid and liquid-solid phase boundary is approached. We have also examined the change of configurational energy with temperature. The slope of configurational energy as a function of temperature changes at the phase boundary. The transition temperatures, at which this slope changes, are estimated to be $T=1920$, 2000, 2620, and 3240 K for the densities quoted above. One can draw a crude freezing line based on these points (see the dotted line in Fig. 2). The error bar in temperature is estimated to be about ± 100 K. The comparison with the HMSA freezing line, also reported in Fig. 2, shows only semiquantitative agreement between theory and simulation since, at fixed temperature, the two lines appear shifted from each other by about 10% in density. The discrepancy is puzzling but might be due to the different criteria for locating the transition temperature used in these two methods.

In the low density region, liquid C_{60} coexists with vapor. Pair distribution functions and mean-square displacements are not a sensitive way to distinguish the liquid from the gas. Again, the time-dependent trajectory plots and change of configurational energy have been used to locate the vapor-liquid coexisting region since the single fluid phase and vapor-liquid coexistence region behave differently. The transition temperatures estimated for the heating runs at $\rho=0.224$, 0.391, 0.559, 0.754, 0.944, and 0.964 nm^{-3} are also shown in Fig. 2 by the squares with vertical error bars. They likely provide upper limits to the coexistence region. The HMSA liquid-vapor coexistence line, obtained through the procedure outline in Ref. [14] is also reported in Fig. 2. The inset reports the HMSA T-P freezing line, and liquid-vapor coexistence line, respectively. Again, theory and simulation are in semiquantitative agreement with each

other. The HMSA critical point estimated by interpolating the gas and liquid branch is $T \approx 2050$ K and $\rho_c \approx 0.56$ nm^{-3}. The MD data suggest a value close to 1900 K.

We have also employed a block density distribution technique [17,18] in order to estimate the densities of vapor and liquid in their phase coexistence region in an effect to confirm the above results. To analyze the constant-volume simulation data the simulation box was, therefore, divided into smaller blocks. The density in each block is estimated and the ensemble average of the probability distribution of the block density is then evaluated. The probability distribution at the average density $\rho = 0.559$ nm^{-3} has been examined for several temperatures ranging from 1700 to 2500 K. At the lowest temperature the block density distribution is broad and has two prominent peaks, which correspond to the liquid and vapor, respectively. With increasing temperature the two peaks approach each other and eventually merge into one, which suggests that the system has reached a one-phase region. The peak becomes sharper with increasing temperature. From this analysis we estimated the density of gas and liquid at several temperatures and mapped out roughly the boundary of vapor-liquid coexistence region shown in Fig. 2 (squares with crosses representing the error bars). The phase boundary obtained in this fashion is shifted to lower temperature for a given density compared to the previous estimates. This might be due to the relatively small size of the simulation box.

We have carried out constant-pressure MD simulations at pressures $P = 0.022$ and 0.5 kbar. The simulations were started from a fcc solid phase at $T = 1500$ K. The systems were then heated up gradually. The peak position in $g(r)$ plots clearly reveal the isobaric thermal expansion of the lattice. Eventually, we observe a strong expansion and large fluctuations of the simulation box; behavior which signals that the system is in the liquidlike region. The simulation code we employed prevented us from carrying out a detailed study of the melting region [19]. The solid phase is stable up to 2320 K for $P = 0.022$ kbar, and 2570 K at $P = 0.5$ kbar. The corresponding fcc lattice constants are 15.00 and 14.99 Å, respectively. These two constant-pressure simulations give us a crude estimate of the melting transition (mechanical instability [19]), and are shown in Fig. 2 as crosses. According to the HMSA calculation, the triple point pressure is $P = 14$ bars. Unfortunately, it is not possible for us to distinguish zero pressure from the triple point value within the resolution of the MD simulations.

In many ways one might expect high temperature C_{60} to be similar to a Lennard-Jones system. A comparison of Girifalco's C_{60} potential with the Lennard-Jones (12-6) potential is, therefore, of interest. For the Lennard-Jones (12-6) system it is widely agreed that $T_{\text{triple}}/\epsilon = 0.66$ with $\rho_{\text{triple}}\sigma^3 = 0.86$, and $T_c/\epsilon = 1.3$ with $\rho_c\sigma^3 = 0.304$ [9–11]. One can fit the observed cohesive energy, $\Delta H = 167.8$ kJ/mol [20], and nearest neighbor distance $R_{NN} = 10.05$ Å [8] of fcc C_{60} to a Lennard-Jones potential acting between the center of mass of the molecules and obtain a well depth, $\epsilon_{LJ} = 2330$ K and $\sigma_{LJ} = 9.22$ Å. From these parameters, the scaling of Lennard-Jones values gives $T_{\text{triple}} = 1540$ K, $\rho_{\text{triple}} = 0.86/\sigma_{LJ}^3 = 1.097$ nm^{-3} and similarly, $T_c = 3030$ K and $\rho_c = 0.304/\sigma_{LJ}^3 = 0.388$ nm^{-3}. The integral-equation results, $T_{\text{triple}} = 1774$ K and $\rho_{\text{triple}} = 0.944$ nm^{-3}, are not very different from the above estimates. However, the critical parameters estimated from the MD simulations, $T_c \approx 1900 \pm 100$ K and $\rho_c = 0.56 \pm 0.06$ nm^{-3} and HMSA, $T_c \approx 2050$ K and $\rho_c = 0.56$ nm^{-3} differ dramatically from the prediction based on scaling the Lennard-Jones values. The character of the C_{60} intermolecular interaction may be responsible for the seemingly different behavior. In particular, the repulsive wall of the C_{60} potential is much stiffer than that of a Lennard-Jones potential and the attractive region of the C_{60} interaction damps off rather faster.

To summarize, we report a preliminary investigation of the phase diagram of high temperature C_{60} using both integral-equation and molecular dynamics simulations methods based on rigid molecules interacting via the Girifalco sphericalized pontential. The results obtained from these two approaches are reasonably consistent. This work suggests that for rigid C_{60} molecules the liquid would only be observed in a narrow temperature range compared with a Lennard-Jones system. The nature of the critical point is still somewhat uncertain. It would be of great interest to apply the Gibbs ensemble method to this model system [11] to check whether or not our rough predictions concerning the critical point for the model are confirmed. Unfortunately, the predicted temperature range for both liquid and dense fluid ($T > 1800$ K) is disappointingly high. In fact, it is above the temperature at which C_{60} has been reported to polymerize [21].

Both A.C. and M.L.K. thank the NSF for support and Rick Smalley for his interests in this calculation. C.C. acknowledges the support of MURST through Consorzio Interuniversitario Fisica della Materia. This project began when C.C. was a NATO Fellow at University of Pennsylvania. We thank Daan Frenkel for helpful discussions.

Note added.— After submitting this manuscript we became aware of a related investigation dealing with the possible existence of liquid C_{60} [22]. The simulation results are in broad agreement with the present investigation. However, they conclude on the basis of free energy calculations that the sublimation line passes close to but above the metastable critical point and that the liquid does not exist.

[1] W. Krätschmer, L. D. Lamb, K. Fostiropoulos, and D. R. Huffman, Nature (London) **347**, 354 (1990).

[2] P. A. Heiney, J. E. Fischer, A. R. McGhie, W. J. Romanow, A. M. Denenstein, J. P. McCauley, Jr., A. B. Smith III, and D. E. Cox, Phys. Rev. Lett. **66**, 2911 (1991); R. Sachidanandum and A. B. Harris, Phys. Rev. Lett. **67**, 1467 (1991).
[3] W. I. F. David, R. M. Ibberson, J. C. Matthewman, K. Prassides, T. J. S. Dennis, J. P. Hare, H. W. Kroto, R. Taylor, and D. R. M. Walton, Nature (London) **353**, 147 (1991); W. I. F. David, R. M. Ibberson, T. J. S. Dennis, J. P. Hare, and K. Prassides, Europhys. Lett. **18**, 219 (1992).
[4] R. Tycko, G. Dabbagh, R. M. Fleming, R. C. Haddon, A. V. Makhija, and S. M. Zahurak, Phys. Rev. Lett. **67**, 1886 (1991).
[5] M. Sprik, A. Cheng, and M. L. Klein, J. Chem. Phys. **96**, 2027 (1992).
[6] N. W. Ashcroft, Europhys. Lett. **16**, 355 (1991).
[7] G. Zerah and J. P. Hansen, J. Chem. Phys. **84**, 2336 (1985).
[8] L. A. Girifalco, J. Phys. Chem. **95**, 5370 (1992); **96**, 858 (1992).
[9] J.-P. Hansen and L. Verlet, Phys. Rev. **184**, 151 (1969).
[10] J. Q. Broughton and G. H. Gilmer, J. Chem. Phys. **79**, 5095 (1983).
[11] A. Z. Panagiotopoulos, Mol. Phys. **61**, 813 (1987).
[12] A. Cheng and M. L. Klein, J. Chem. Phys. **95**, 6750 (1991); Phys. Rev. B **45**, 1889 (1992).
[13] M. C. Abramo and C. Caccamo, Phys. Lett. A **166**, 70 (1992).
[14] C. Caccamo, P. V. Giaquinta, and G. Giunta, J. Phys. Condens. Matter **5**, Suppl. 33B, B75 (1993).
[15] P. V. Giaquinta and G. Giunta, Physica (Amsterdam) **187A**, 145 (1992).
[16] P. V. Giaquinta, G. Giunta, and S. Prestipino Giarritta, Phys. Rev. A **45**, 6966 (1992).
[17] M. Rovere, D. W. Hermann, and K. Binder, Europhys. Lett. **6**, 585 (1988); M. Rovere, D. W. Heermann, and K. Binder, J. Phys. Condens. Matter **2**, 7009 (1990).
[18] D. Marx, P. Nielaba, and K. Binder, Phys. Rev. Lett. **67**, 3124 (1991).
[19] D. K. Chokappa and P. Clancy, Mol. Phys. **61**, 597 (1987).
[20] C. Pan, M. P. Sampson, Y. Chai, R. H. Hauge, and J. L. Margrave, J. Chem. Phys. **95**, 2944 (1991).
[21] A. M. Rao, P. Zhou, J-A. Wang, G. T. Hager, J. M. Holden, Y. Wang, W.-T. Lee, X.-X. Bi, P. C. Eklund, D. S. Cornett, M. A. Duncan, and I. J. Amster, Science **259**, 955 (1993).
[22] M. H. J. Hagen, E. J. Meijer, G. C. A. M. Mooij, D. Frenkel, and H. N. W. Lekkerkerker (to be published).